Molecular Simulation
Vol. 34, Nos. 10–15, September–December 2008, 1149–1158

Taylor & Francis
Taylor & Francis Group

On the mechanical properties and auxetic potential of various organic networked polymers

Joseph N. Grima*[1], Daphne Attard, Richard N. Cassar, Luke Farrugia, Lara Trapani and Ruben Gatt

Department of Chemistry, University of Malta, Msida, Malta

(*Received 3 February 2008; final version received 29 September 2008*)

We simulate and analyse three types of two-dimensional networked polymers which have been predicted to exhibit on-axis auxetic behaviour (negative Poisson's ratio), namely (1) polyphenylacetylene networks that behave like flexing re-entrant honeycombs, commonly referred to as 'reflexynes', (2) polyphenylacetylene networks that mimic the behaviour of rotating triangles, commonly referred to as 'polytriangles' and (3) networked polymers built from calix[4]arene units. More specifically, we compute and compare their in-plane off-axis mechanical behaviour, in particular their off-axis Poisson's ratios and show that in some cases, the sign and magnitude of the Poisson's ratio are dependent on the direction of loading. We propose two functions that can provide a measure for the extent of auxeticity for such anisotropic materials and show that the polytriangles are predicted as the most auxetic when compared with the other networks with the reflexyne re-entrant networks being the least auxetic.

Keywords: auxetic; negative Poisson's ratios; mechanical properties; networked polymers

1. Introduction

Materials with negative Poisson's ratios, more commonly known as auxetics [1], exhibit the anomalous property of expanding laterally when stretched and contracting laterally when compressed [1,2]. This behaviour is in sharp contrast to that of 'normal' everyday (conventional) materials for which Poisson's ratios are positive with a value usually lying within the range of 0.25–0.33 [3].

Although auxetics are not commonly encountered in everyday life, in recent years there has been considerable research into this field in view of their very useful properties [4]. This led to the discovery of numerous auxetic materials [1,2,5–41], ranging from synthetic polymeric foams [10–16] to naturally occurring silicates and zeolites [17–31]. Additionally, a number of auxetic models and structures have also been identified [42–56].

In all of the above cases, auxeticity can be explained in terms of the geometry of the system and the way this geometry changes when the system is subjected to uniaxial loads (deformation mechanism). For example, Poisson's ratios in the naturally occurring silicate α-cristobalite and in various zeolites have been explained using models based on connected rigid units which, when loaded in tension, rotate relative to each other to form a more open structure [27,28,42,50], while the auxeticity in the liquid-crystalline polymers synthesised by Griffin et al. [33,34] and Aldred and Moratti [35] has been attributed to a model involving the rotation of laterally attached rods.

It is important to note that although naturally occurring materials have the obvious advantage that there is no need for synthesis, man-made auxetics offer the benefit that their macroscopic properties may be tailor-made to exhibit a specific predetermined profile of mechanical properties, thus making them better suited for particular applications. One approach for designing man-made molecular-level auxetics is to have a molecular structure that mimics the properties of another auxetic system, for example a naturally occurring auxetic or an auxetic macrostructure. Downscaling of macrostructures to the molecular level, a technique first used in the pioneering work by Evans et al. [1], is possible because the Poisson's ratio is a scale–independent property, i.e. it is normally unaffected by the scale at which a particular 'deformation mechanism' operates. In this respect, it should be noted that if a geometry-based model for the behaviour of a system is available, then this model can be used as a guide for fine-tuning the design and synthesis of molecular auxetics.

In this paper, we use the commercially available molecular modelling package Materials Studio® V4.2 (Accelrys Inc., San Diego, CA, USA) to re-examine a number of 'auxetic' two-dimensional molecular networks that have been designed through the downscaling technique, namely:

(1) 'reflexyne' polyphenylacetylene networks (Figure 1(a)), originally reported by Evans et al. [1], which mimic the behaviour of auxetic re-entrant honeycombs (Figure 2(a)),
(2) 'polytriangles' polyphenylacetylene networks (Figure 1(b)), originally reported by Grima and Evans [6], which mimic the behaviour of rotating triangles (Figure 2(b)), and

*Corresponding author. Email: joseph.grima@um.edu.mt

ISSN 0892-7022 print/ISSN 1029-0435 online

DOI: 10.1080/08927020802512187
http://www.informaworld.com

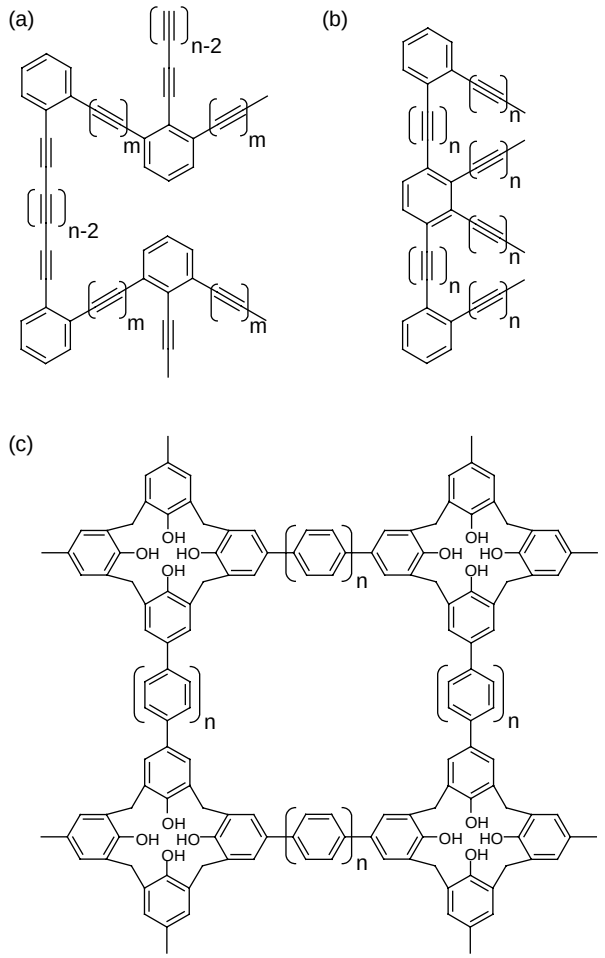

Figure 1. An idealised two-dimensional representation of the systems modelled in this paper: (a) the reflexynes **1A**–**C**, where for **1A**, **1B** and **1C** $(m,n) = (1,4)$, (1,5) and (1,6), respectively, (b) the polytriangles **2A**–**C**, where for **2A**, **2B** and **2C**, $n = 3$, 4 and 5, respectively, and (c) the polycalixes **3A**–**C**, where for **3A**, **3B** and **3C**, $n = 0$, 1 and 2, respectively.

(3) polymers built from calix[4]arenes (Figure 1(c)) (henceforth referred to as 'polycalixes'), originally reported by Grima et al. [7,8], which mimic the behaviour of an 'egg rack' macrostructure which when loaded in tension, opens up in all directions like an umbrella (Figure 2(c) and (d)), hence producing a negative Poisson's ratio in the plane of the structure.

In particular, we assess how these systems behave when they are loaded in an in-plane off-axis direction in an attempt to determine which of these systems is most capable of exhibiting auxetic behaviour.

2. Simulations

Force-field-based simulations were carried out using the commercially available software package Materials Studio, V4.2 (Accelrys Inc.) on nine systems illustrated in Figure 1, in particular three reflexynes (**1A**–**C**, see Figure 1(a) with $(m,n) = (1,4)$, (1,5) and (1,6), respectively), three polytriangles (**2A**–**C**, see Figure 1(b) with $n = 3$, 4 and 5, respectively) and three polycalixes (**3A**–**C**, see Figure 1(c) with $n = 0$, 1 and 2, respectively). These systems, which have all been modelled before using different force-fields in an attempt to obtain their on-axis Poisson's ratio and Young's moduli [5,6,8,9], have been chosen as they represent a representative sample of each class of materials.

These systems were build as infinite crystalline systems (Figure 1) with the plane of interest aligned in the (1 0 0) plane. In the third direction, the networks were allowed to stack freely 'on each other' (in the case of the reflexynes and the polytriangles) or 'inside one another' (in the case of the polycalixes). The crystals were oriented in the global *XYZ*-space in such a way that the [0 0 1] direction was always parallel to the *Z*-axis with the [0 1 0] direction lying in the *YZ*-plane. This alignment was chosen so as to ensure that the plane of the networks remains parallel to the *YZ*-plane and to enable a direct comparison with earlier work by Grima and Evans [6], and Grima et al. [7,8] performed using Cerius^2 (Accelrys Inc.).

Energy expressions for each of these nine networks were set up through the Discover Simulation Engine within Materials Studio 4.2 (henceforth referred to as MS Discover) using parameters from the PCFF [57] force-field^2 with non-bond terms being added using the Ewald summation technique [58]. Note that the PCFF force-field was chosen in preference to the DREIDING force-field that was used in the earlier studies on the reflexynes [9] and the polytriangles [6] in view of the fact that unlike the PCFF force-field, the DREIDING force-field is unable to correctly represent the C_{4v} symmetry which is characteristic of single calix[4]arenes.

An energy minimisation was then performed to the default MS Discover ultra-fine convergence criteria using the SMART minimiser as implemented in MS Discover.[3] During the minimisation, all cell parameters were set as variables, i.e. no constraints on the shape and size of the unit cell were applied.

The 6×6 stiffness matrix $\mathbf{C}$, which relates the stress $\boldsymbol{\sigma}$ and the strain $\boldsymbol{\varepsilon}$ through $\boldsymbol{\sigma} = \mathbf{C}\boldsymbol{\varepsilon}$, was then simulated using the constant strain method found in the Materials Studio V4.2 Forcite module (henceforth referred to as MS Forcite). In these simulations, the maximum strain amplitude was set to 0.003, i.e. 0.3% strain and seven distorted structures were generated for each strain pattern. Note that in such simulations, the maximum strain amplitude should be in the range of 0.1–1% in an attempt to ensure that the strains are small enough to permit the structure to behave within its region of linear elasticity and at the same time avoid a situation, where the strains are so low that the simulations generate a set of structures that are very similar to one another, in which case computational

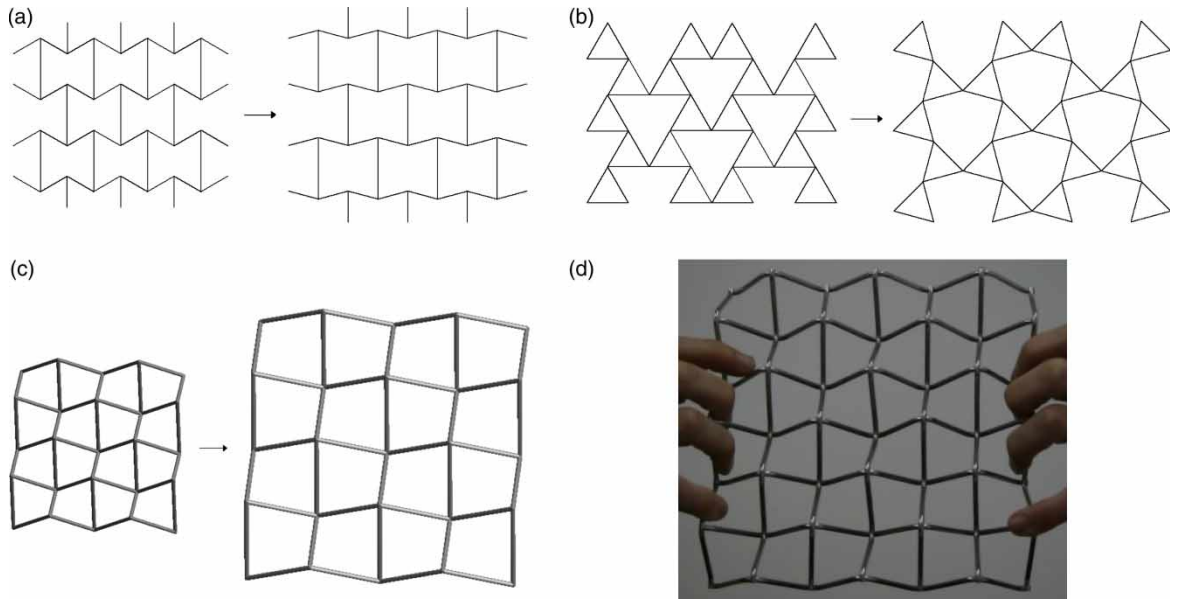

Figure 2. (a)–(c) Examples of models/mechanisms exhibiting auxetic behaviour: (a) auxeticity from hinging re-entrant honeycombs, (b) auxeticity from rotating hinging triangles, and (c) auxeticity from the 'egg rack'/'opening of an umbrella' mechanism (The 'egg rack' on which this system is based is shown in (d).) Animations of Figure 2(a)–(c) are given as Supplementary Information, available online.

noise may become significant when comparing their calculated stress values.

The in-plane on-axis Poisson's ratios and moduli from these systems were then calculated from the compliance matrix $\mathbf{S} = \mathbf{C}^{-1}$, which for the *YZ*-plane (the plane of the networks) are given by:

$$\text{Young's moduli}: \quad E_y = \frac{1}{s_{22}} \quad E_z = \frac{1}{s_{33}},$$

$$\text{Poisson's ratios}: \quad \nu_{yz} = -\frac{s_{32}}{s_{22}}; \quad \nu_{zy} = -\frac{s_{23}}{s_{33}},$$

$$\text{Shear moduli}: \quad G_{yz} = \frac{1}{s_{44}},$$

while the off-axis properties can be obtained after the stiffness matrices are transformed using appropriate axis transformation techniques [59].

3. Results and discussion

3.1 The simulated structures at zero stress

The simulations suggest that the minimum energy conformations of all the molecular network models possess a shape, which is similar to the idealised structure that they are meant to mimic (Figure 3). We note that in all systems, the favourable $\pi-\pi$ interactions between the different layers are being well represented. In fact, for polyphenylacetylene networks, the minimum energy separation between the different layers down the third direction is approximately 3.28 Å in the case of the reflexynes (Figure 3(a)) and approx. 3.44 Å in the case of polytriangles (Figure 3(b)), while, in the polycalixes we find that, for example, the distance between parallel layers of calix[4]arenes in **3A** is 3.38 Å (Figure 3(c)). These separations are comparable with the distance between layers of graphite (3.35 Å) [60]. We also note that in general, stacking in the third dimension is in such a way that whenever possible, the centres of the benzene rings are offset from one another, this being clearly indicated by the deviations in the unit cell angles β and γ from 90° in the case of the polyphenylacetylene networks (Figure 4). It is also interesting to note that the (1,4)-reflexyne molecular network **1A** is significantly non-planar with the phenyl rings adopting a conformation, where they are at an angle to the *YZ*-plane (the 'plane of the networks') as illustrated in Figure 3(a), once again, in an attempt to optimise the favourable $\pi-\pi$ interactions between the spatially adjacent phenyl rings in the system.

3.2 The simulated on-axis Poisson's ratios and moduli

The on-axis Poisson's ratios and moduli as simulated in this study by the PCFF force-field are summarised in Table 1, where they are compared with the equivalent published data obtained using the DREIDING force-field in the case of the reflexynes [5,9] and polytriangles [6] and the PCFF force-field found within Cerius[2] in the case of the polycalixes [8].

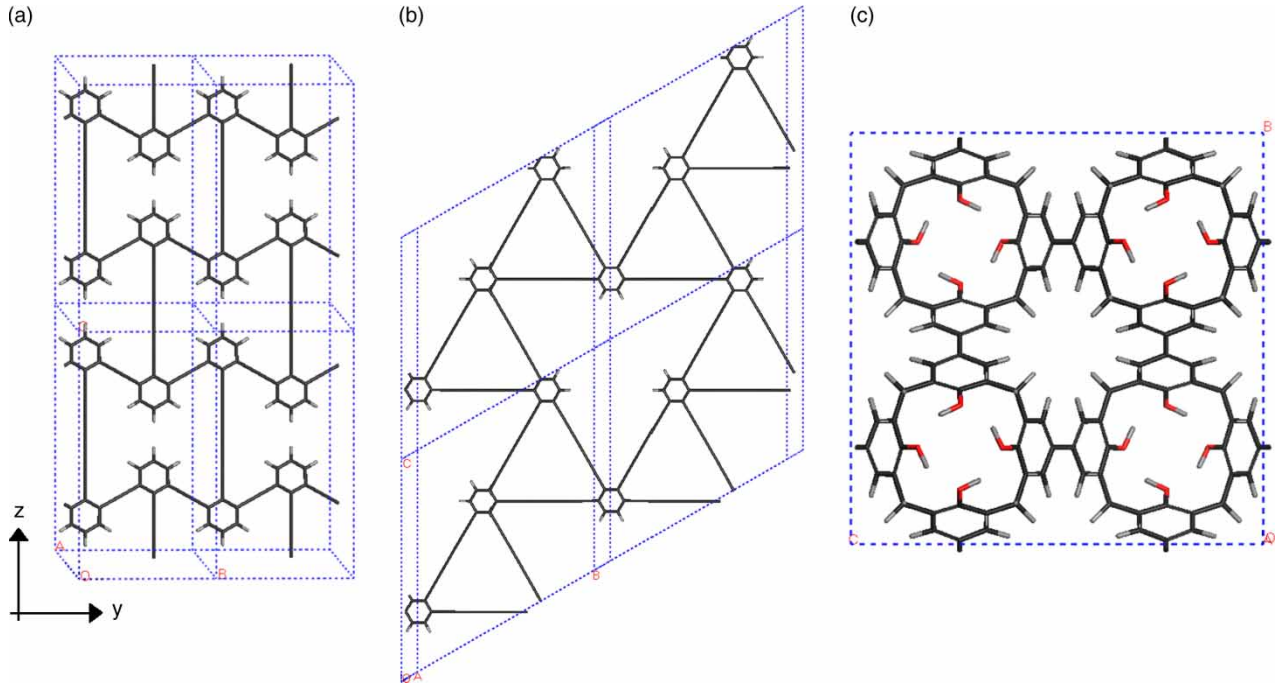

Figure 3. The projections in the *YZ*-plane of the minimum energy conformations of (a) **1A**, (b) **2A** and (c) **3A**. Note that for clarity, the bond order is not shown.

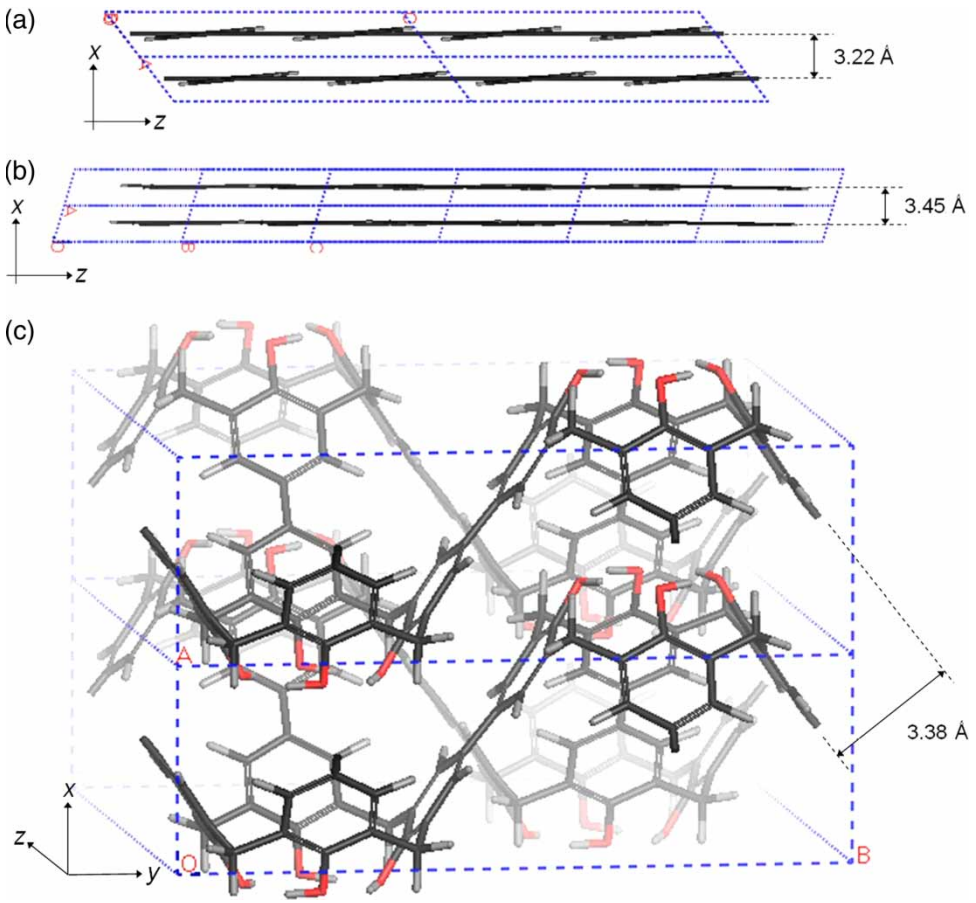

Figure 4. Images showing the stacking down the third dimension for (a) **1A**, (b) **2A** and (c) **3A**. Note that in all cases, the stacking suggests that the $\pi-\pi$ interactions are being well represented.

Table 1. The on-axis mechanical properties of reflexynes (**1A–C**), polytriangles (**2A–C**) and 'double calixes' (**3A–C**) obtained using the PCFF force-field found in Materials Studio compared with the values obtained from literature (when available).

	Method	ν_{yz}	ν_{zy}	E_y (GPa)	E_z (GPa)	G_{yz}	Density (g/cm^3)
1A	PCFF	−0.41	−0.34	120.05	99.38	4.57	1.20
	Evans et al. [9]	*− 0.29*	*− 0.29*	*124*	*110*	–	–
	Alderson et al. [5]	–	–	–	–	–	–
1B	PCFF	−0.37	−0.41	92.68	101.71	3.64	1.02
	Evans et al. [9]	*− 0.29*	*− 0.39*	*95*	*116*	–	–
	Alderson et al. [5]	*− 0.33*	*− 0.39*	*94*	*110*	–	–
1C	PCFF	−0.31	−0.46	78.20	114.25	2.65	0.92
	Evans et al. [9]	*− 0.22*	*− 0.42*	*84*	*140*	–	–
	Alderson et al. [5]	*− 0.28*	*− 0.44*	*80*	*124*	–	–
2A	PCFF	−0.51	−0.51	52.56	52.60	53.52	0.90
	Grima & Evans [6]	*− 0.83*	*− 0.83*	–	–	–	–
2B	PCFF	−0.65	−0.65	31.51	31.48	45.50	0.75
	Grima & Evans [6]	*− 0.90*	*− 0.90*	–	–	–	–
2C	PCFF	−0.75	−0.75	20.18	20.12	39.75	0.64
	Grima & Evans [6]	*− 0.94*	*− 0.93*	–	–	–	–
3A	PCFF	−0.47	−0.47	18.79	18.79	4.61	1.42
	Grima et al. [8]	−0.51	−0.51	*18.10*	*18.10*	–	–
3B	PCFF	−0.86	−0.86	3.65	3.65	1.95	1.10
	Grima et al. [8]	*− 0.87*	*− 0.85*	*3.78*	*3.78*	–	–
3C	PCFF	−0.95	−0.87	1.67	1.52	0.99	0.89
	Grima et al. [8]	*− 0.93*	*− 0.88*	*1.67*	*1.58*	–	–

When analysing these results, we note that in the case of the polycalixes, the simulations carried out by Materials Studio were in excellent agreement with the simulations performed using the same force-field as found in Cerius[2], thus confirming that the mechanical properties calculation tools found in the Forcite module of Materials Studio are well implemented. The small deviations obtained are to be expected in view of the fact that the energy minimisation process depends on both the minimisation algorithm chosen and on the initial direction that the minimiser takes, and thus minor differences can arise when a minimisation is repeated.

In the case of the polyphenylacetylene networks **1A–C** and **2A–C**, we note that our simulations confirm the predictions made in the previous studies using the DREIDING force-field that all of these systems exhibit negative on-axis Poisson's ratios in the plane of the networks (the *YZ*-plane). It is also interesting to note that although for a given structure, the different force-fields fail to agree on the actual values of Poisson's ratios, a result which could be expected given that the properties are being calculated using different force-fields, the main trends in the results are still being represented, such as the observation that in the case of the polytriangles, the auxeticity increases as the acetylene chains are made longer. This agreement between the two sets of results is very significant as it indicates that the results predicted are not artefacts of some particular force-field, thus giving additional confidence in the quality of the simulated properties presented here.

When we compare the magnitude of results obtained by the different types of networks, something which is now possible since the three types of networks are simulated using the same force-field through the same protocol, we observe that despite the differences in the geometry of the systems modelled, the results *prima facie* suggest that all the three types of systems have a comparable potential to exhibit negative on-axis Poisson's ratios. In fact, in all cases, on-axis Poisson's ratio ranges between −0.31 and −0.95, the actual values depending on the exact shape or size of the system being modelled. For example, we find that according to the PCFF force-field, ν_{zy} for **1C**, **3A** and **2A** is predicted as −0.46, −0.47 and −0.51, respectively, despite the obvious differences between these systems.

If we now look at on-axis Young's and shear moduli for the different networks, we note that once again the trends suggested by the earlier simulations are reproduced. In particular, we note that in the case of the polytriangles and polycalixes, the moduli decrease as the size of the triangles or 'arm' lengths of the calixes increase (density decreases). This is expected since in general, from a mechanistic point of view, an increase in the 'arm' length leads to larger induced moments when a force is applied to the system, leading to a higher extent of deformation that

is reflected in a decrease in Young's and shear moduli. In the case of the reflexynes, the situation is more complex as we find that while the on-axis Young's modulus in the *Y*-direction and shear modulus increase with a decrease in *n* (the number of triple bonds in the vertical acetylene chain aligned with the *Z*-direction), the Young's modulus in the *Z* direction decreases. Such variations were predicted by Gibson and Ashby's mechanical model [53] (*m*, *n* in our molecular model may be mapped to the variables *l* and *h*, respectively, in Gibson and Ashby's model).

It is also interesting to note that the on-axis shear moduli of the polytriangles are considerably larger than those of the other systems, a property which arises from the fact that triangles are structurally difficult to shear. In this respect, it is important to note that the analytical model for the idealised 'rotating hinging triangles' suggests that the shear modulus of such systems is infinite [55], a property that in molecular level systems is difficult to accomplish.

These high on-axis shear moduli are however only limited to the polytriangles. In fact we find that despite the fact that re-entrant honeycombs have very high on-axis Young's moduli, they are very weak in shear. For example, in the case of the molecular-level honeycomb (1,4)-reflexyne (**1A**), G_{yz} is only 3.81% of E_y and 4.60% of E_z. The weakness of these honeycombs when subjected to an on-axis shear strain is not limited to the reflexyne molecular honeycomb networks but is a property of all such honeycombs, irrespective of the scale at which they are built. In fact, this weakness in shear is also inferred by Gibson and Ashby's analytical equations for the idealised flexing models which predict that for a flexing re-entrant honeycomb having dimensions *t*/*l* and *h*/*l* of 0.01 and 2, respectively, and a re-entrant angle of 30° (dimensions defined in Figure 6(b)), the on-axis shear modulus is only 3.75% of the Young's moduli.

3.3 *The off-axis mechanical properties*

Plots of the in-plane (*YZ*-plane) off-axis Poisson's ratios and moduli for the nine different systems are shown in Figure 5. These plots very clearly show that because of their distinct geometries and symmetries, off-axis Poisson's ratio profiles of these systems are in fact very different from each other. (Note that although there is extensive work that discusses the on-axis properties of molecular reflexyne, polytriangles and polycalix networks, and there is also work that discusses the off-axis mechanical properties of idealised flexing/hinging/stretching re-entrant honeycombs [61] and idealised 'rotating triangles' [55], no analysis of the off-axis properties of the molecular networks has yet been presented.)

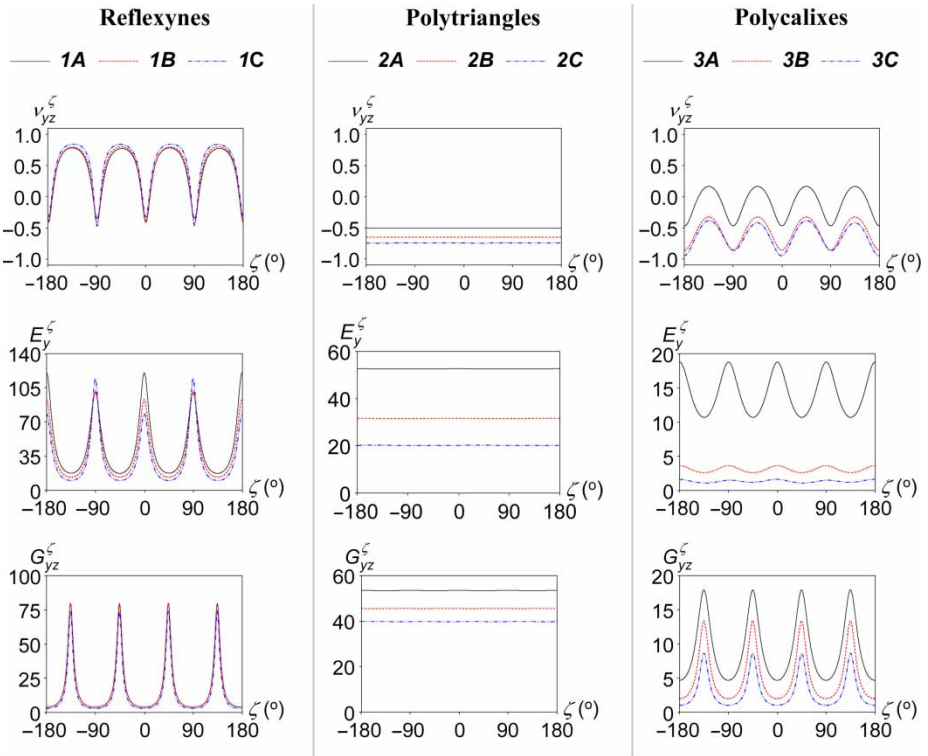

Figure 5. Off-axis plots for in-plane Poisson's ratios, ν_{yz}, Young's moduli E_y and shear moduli G_{yz} for each of the network systems considered as obtained by the PCFF force-field.

In particular, for the Poisson's ratio, we observe that:

(1) In the case of the reflexynes, the off-axis plots are characterised by non-auxetic behaviour, having very high positive off-axis Poisson's ratios, the maximum of which is *ca*. 0.85 and corresponds approximately to loading at 45° to the *Y*- and *Z*-directions.
(2) In the case of the polytriangles, off-axis Poisson's ratios are always negative and very similar to those observed on-axis (the networks are *quasi*-isotropic), as expected from systems exhibiting hexagonal symmetry.
(3) In the case of the polycalixes, off-axis Poisson's ratios are less negative than on-axis. However, in the case of **3B** and **3C**, in-plane auxeticity can be observed for loading in any direction of the plane, and in the case of **3A**, the system is auxetic for loading in most, but not all, directions.

In an attempt to quantify these observations regarding the extent of in-plane auxeticity of the different systems, we shall define two properties, namely:

(a) The 'auxetic probability', $P_{\text{aux}}[YZ]$, a function which may be defined as:

$$P_{\text{aux}}[YZ] = \frac{1}{2\pi}\int_0^{2\pi} H_{YZ}(\zeta)\ \mathrm{d}\zeta,$$

where

$$H_{YZ}(\zeta) = \begin{cases} 1 & \text{if } \nu_{yz}^{\zeta} < 0 \\ 0 & \text{if } \nu_{yz}^{\zeta} \geq 0 \end{cases}$$

which gives a measure of the probability that in-plane Poisson's ratio is negative for loading in an arbitrary direction in the plane. This value can range from 0 to 1, where a value of 0 suggests that the system is conventional for loading in all directions while a value of 1 indicates that the system is auxetic for loading in all directions.

(b) 'Average in-plane Poisson's ratio', $\bar{\nu}[YZ]$, which may be defined as:

$$\bar{\nu}[YZ] = \frac{1}{2\pi}\int_0^{2\pi} \nu_{yz}^{\zeta}\ \mathrm{d}\zeta$$

a property which gives a measure of average Poisson's ratio in the plane.

When these properties are evaluated for the different networks (Table 2), we note that, starting with the most auxetic system, the order of auxeticity in the *YZ*-plane is:

(a) If we classify them according to the magnitude of $P_{\text{aux}}[YZ]$:

$$\{\mathbf{2A-C}, \mathbf{3B}, \mathbf{3C}\} > \mathbf{3A} > \mathbf{1A} > \mathbf{1B} > \mathbf{1C}.$$

(b) If we classify them according to the magnitude of $\bar{\nu}[YZ]$:

$$\mathbf{2C} > \mathbf{2B} > \mathbf{3C} > \mathbf{3B} > \mathbf{2A} > \mathbf{3A} > \mathbf{1A} > \mathbf{1B} > \mathbf{1C}.$$

This analysis clearly suggests that the polytriangles are the best systems in terms of the in-plane off-axis auxeticity, followed by the polycalixes and then by the reflexynes that are in fact predominantly conventional for loading off-axis.

Before we conclude our discussion on the Poisson's ratio, it is important to highlight that although the ranking above suggests that the different systems within the same class have a different extent of auxeticity, this variation is not always explainable in terms of the idealised mechanical model they are meant to mimic. For example, the idealised 'rotating triangles' model [55] predicts constant isotropic Poisson's ratio of -1, something which is clearly not demonstrated by the molecular-level model. This deviation may be explained from the fact that these molecular-level networks are more complex, even in shape, when compared with the idealised model, and while in the idealised 'flexing rotating triangles' model, the sides of the triangles are simple beams, in the case of the molecular-level networks they are two benzene rings joined together by an acetylene chain. In such systems, it is primarily the acetylene chains, especially the longer ones, which behave in a similar way to beams, and hence, in the smaller systems, the deviations from the idealised scenario of Poisson's ratio of -1 are more significant, thus contributing to the observed trend in the Poisson's ratio of **2A–C**. Furthermore, it is important to note that the molecular-level systems are characterised by non-bond interactions that caused the different 'beams' in the systems to interact with each other. Such non-bond interactions are inversely proportional to r^k, where r is the separation of the two interacting atoms, i.e. the extent of interactions increases as the separation between the atoms involved decreases. This will result in a scenario where the denser systems will have more of these non-bond interactions per unit volume than the less dense systems

Table 2. The 'auxetic probability' $P_{\text{aux}}[YZ]$ and 'average in-plane Poisson's ratio' $\bar{\nu}[YZ]$ for the nine networks modelled.

	1A	**1B**	**1C**	**2A**	**2B**	**2C**	**3A**	**3B**	**3C**
$P_{\text{aux}}[YZ]$	0.17	0.16	0.13	1	1	1	0.58	1	1
$\bar{\nu}[YZ]$	0.47	0.50	0.55	−0.51	−0.65	−0.75	−0.11	−0.57	−0.64

thus, once again, resulting in greater deviations from the idealised scenario of Poisson's ratio of -1 in the smaller systems when compared with the larger systems thus resulting. All this results in the observed trend in Poisson's ratios of **2A**–**C**, where we find that **2A** (the smaller system) is the least auxetic and **2C** (the larger and less dense system) being the most auxetic.

It is also interesting to note that although all the 'polycalixes' are auxetic, they do not have in-plane on-axis Poisson's ratio of -1 as predicted by the idealised model [8]. These discrepancies may be explained using similar arguments, i.e. that the smaller systems deviate more from the idealised model they are meant to mimic than the larger systems. In particular, as explained elsewhere [8], we note that the idealised 'egg-rack/umbrella' model is not a very accurate representation of the 'double calix' systems. In fact we note that these systems bear a greater resemblance to structures whose joints are replaced by rhombic units (see Ref. [8] for a more detailed discussion and illustration) in which case we can identify two deformation mechanisms when the system is subjected to an external load. The first of these mechanisms, which acts on the 'arms' of the system, opens the structure, in a similar way to the opening of an umbrella, to flatten out the whole structure, thereby contributing to a negative Poisson's ratio. The second one is the deformation of the rhombi leading to a positive Poisson's ratio. These two opposing mechanisms act concurrently so that net Poisson's ratios for 'polycalixes' are less negative than expected. The actual values of the Poisson's ratio depend on the relative magnitude of the mechanisms, which depends on the relative size of the rhombi when compared with the arms (the larger the rhombi, the more they contribute to the overall deformation). From this analysis, one would expect that the smaller systems (where the rhombi are more predominant) to be less auxetic than the larger systems (where the umbrella arms are more predominant). This trend is in fact evident in results obtained in this study, where **3A** is found to be much less auxetic than **3C**.

If we now look at the in-plane off-axis moduli of these systems (Figure 5), we note that while the moduli of the polytriangles are unaffected by the direction of loading, those of the reflexynes and the polycalixes are characterised by a high degree of anisotropy. In particular, we note that high Young's moduli observed in the reflexyne for on-axis loading decrease sharply for loading off-axis to values that are about a fifth of their on-axis values. Furthermore, it is interesting to note that the highly auxetic polytriangles and polycalixes are very distinct from each other in the sense that the in-plane moduli of the polytriangles are consistently higher than the in-plane moduli of the polycalixes, despite the fact that the polycalixes are significantly denser than the polytriangles (Table 1). All this suggests that the polytriangles may be better suited than the other networks, particularly the reflexynes, in applications that simultaneously require low density, high auxeticity, high stiffness and/or isotropy in the in-plane properties.

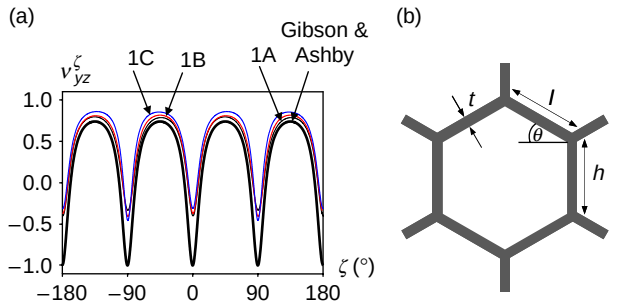

Figure 6. (a) A comparison of off-axis in-plane Poisson's ratio plots obtained in this study for the molecular networks **1A**–**C** with those predicted through the analytical model of Gibson and Ashby [53,54] for a structure made from ABS ($E_s = 2.206$ GPa) and with a t:l ratio of 0.01, a h:l ratio of 2 and a re-entrant angle of 30° (i.e. $\theta = -30°$). Using these values, on-axis Poisson's ratios were both found to be -1 while Young's moduli were found to be 5.095 MPa and the shear modulus 0.191 MPa. (b) The geometrical parameters that define hexagonal honeycombs.

Although the results on the re-entrant honeycombs presented here may *prima facie* appear as surprising, particularly in view of the fact that the re-entrant shape is so closely associated with auxetic behaviour, it is important to note that this lack of off-axis auxeticity in 'flexing re-entrant honeycombs' is consistent with Gibson and Ashby's model of idealised honeycombs [53,54] and results from the fact that such honeycombs are very weak in shear when compared with the uniaxial on-axis stretching, In fact, as illustrated in Figure 6(a), the profile of Poisson's ratio for a re-entrant honeycombs made from ABS having dimensions t/l and h/l of 0.01 and 2, respectively (dimensions defined in Figure 6(b)), is very similar to those of the molecular-level networks.

4. Conclusion

In this work, we have fully characterised and compared the in-plane properties of three types of hypothetical molecular polymeric networks that were predicted to exhibit auxetic behaviour, in particular the polyphenylacetylene networks which, to a first approximation, mimic the behaviour of 'flexing re-entrant honeycombs' or 'flexing rotating triangles', and the polymers built from calix[4]arene building blocks.

We showed that these three types of systems exhibit very different mechanical properties, with the polytriangles being *quasi*-isotropic in the plane of the networks while the other networks, particularly the reflexyne, are highly anisotropic.

We also showed that although for many years it was assumed that auxetic behaviour is primarily obtained from systems having re-entrant honeycomb characteristics, these systems are not the best for obtaining auxetic behaviour due to the fact that they are very weak in shear thus resulting in highly positive off-axis Poisson's ratios. In fact, we showed that the polytriangles and the polycalixes are effectively more auxetic than those based on the re-entrant model, with the polytriangles also benefiting from higher shear moduli when compared with the polycalixes.

We hope that the comparison presented here will be of use to scientists working in the design and synthesis of such molecular-level auxetics by providing them with an 'ordered list' of systems that are most likely to exhibit auxetic behaviour, and also by giving them a better insight into the stiffness that these systems are likely to have.

Acknowledgements

The financial support of the Malta Council for Science and Technology and of the Malta Government Scholarship Scheme (Grant Number ME 367/07/17 awarded to Daphne Attard) is gratefully acknowledged. The authors are also very grateful to Accelrys Inc. for the assistance they provided.

Notes

1. www:http://home.um.edu.mt/auxetic
2. As shown in Table 1, the PCFF force-field can simulate all the systems under consideration allowing for a proper and unbiased comparison between the systems, as discussed later.
3. The SMART minimiser as implemented within MS Discover is a compound minimiser where the minimisation commences with the steepest descent algorithm followed by a conjugate gradient algorithm and terminates with a Newton Raphson algorithm.

References

[1] K.E. Evans, M.A. Nkansah, I.J. Hutchinson, and S.C. Rogers, *Molecular network design*, Nature 353 (1991), p. 124.
[2] R. Lakes, *Foam structures with a negative Poisson's ratio*, Science 235 (1987), pp. 1038–1040.
[3] S.P. Timoshenko and J.N. Goodier, *Theory of Elasticity*, 3rd ed., McGraw-Hill, New York, 1970.
[4] A. Alderson, *A triumph of lateral thought*, Chem. Ind. 10 (1999), pp. 384–391.
[5] A. Alderson, P.J. Davies, M.R. Williams, K.E. Evans, K.L. Alderson, and J.N. Grima, *Modelling of the mechanical and mass transport properties of auxetic molecular sieves: an idealised organic* (*polymeric honeycomb*) *host-guest system*, Mol. Simul. 31 (2005), pp. 897–905.
[6] J.N. Grima and K.E. Evans, *Self expanding molecular networks*, Chem. Comm. 16 (2000), pp. 1531–1532.
[7] J.N. Grima, J.J. Williams, and K.E. Evans, *Networked calix[4]arene polymers with unusual mechanical properties*, Chem. Comm. 32 (2005), pp. 4065–4067.
[8] J.N. Grima, J.J. Williams, R. Gatt, and K.E. Evans, *Modelling of auxetic networked polymers built from calyx[4]arene building blocks*, Mol. Simul. 31 (2005), pp. 907–914.
[9] K.E. Evans, A. Alderson, and F.R. Christian, *Auxetic two-dimensional polymer networks. An example of tailoring geometry for specific mechanical properties*, J. Chem. Soc. Faraday Trans. 91 (1995), pp. 2671–2680.
[10] F. Scarpa, W.A. Bullough, and P. Lumley, *Trends in acoustic properties of iron particle seeded auxetic polyurethane foam*, P.I. Mech. Eng. C-J. Mech. Eng. Sci. 218 (2004), pp. 241–244.
[11] K.E. Evans, M.A. Nkansah, and I.J. Hutchinson, *Auxetic foams–modeling negative Poisson's ratios*, Acta Metall. Mater. 42 (1994), pp. 1289–1294.
[12] C.W. Smith, J.N. Grima, and K.E. Evans, *A novel mechanism for generating auxetic behaviour in reticulated foams: missing rib foam model*, Acta Mater. 48 (2000), pp. 4349–4356.
[13] J.N. Grima, A. Alderson, and K.E. Evans, *An alternative explanation for the negative Poisson's ratio in auxetic foams*, J. Phys. Soc. Jpn. 74 (2005), pp. 1341–1342.
[14] R.S. Lakes and K. Elms, *Indentability of conventional and negative Poisson's ratio foams*, J. Compos. Mater. 27 (1993), pp. 1193–1202.
[15] N. Chan and K.E. Evans, *Indentation resilience of conventional and auxetic foams*, J. Cell. Plast. 34 (1998), pp. 231–260.
[16] J.B. Choi and R.S. Lakes, *Nonlinear analysis of the Poisson's ratio of negative Poisson's ratio foams*, J. Compos. Mater. 29 (1995), pp. 113–128.
[17] A. Yeganeh-Haeri, D.J. Weidner, and J.B. Parise, *Elasticity of alpha-cristobalite–a silicon dioxide with a negative Poisson's ratio*, Science 257 (1992), pp. 650–652.
[18] N.R. Keskar and J.R. Chelikowsky, *Negative Poisson ratios in crystalline SiO_2 from 1st-principles calculations*, Nature 358 (1992), pp. 222–224.
[19] A. Alderson, K.L. Alderson, K.E. Evans, J.N. Grima, and M. Williams, *Modelling of negative Poisson's ratio nanomaterials: deformation mechanisms, structure–property relationships and applications*, J. Metastable Nanocryst. Mater. 23 (2005), pp. 55–58.
[20] A. Alderson and K.E. Evans, *Rotation and dilation deformation mechanisms for auxetic behaviour in the alpha-cristobalite tetrahedral framework structure*, Phys. Chem. Miner. 28 (2001), pp. 711–718.
[21] A. Alderson, K.L. Alderson, K.E. Evans, J.N. Grima, M.R. Willams, and P.J. Davies, *Modelling the deformation mechanisms, structure–property relationships and applications of auxetic nanomaterials*, Phys. Status Solidi B 242 (2005), pp. 499–508.
[22] J.N. Grima, R. Gatt, A. Alderson, and K.E. Evans, *On the origin of auxetic behaviour in the silicate α-cristobalite*, J. Mater. Chem. 15 (2005), pp. 4003–4005, doi: 10.1039/b508098c.
[23] H. Kimizuka, S. Ogata, and Y. Shibutani, *Atomistic characterization of structural and elastic properties of auxetic crystalline SiO_2*, Phys. Status Solidi B 244 (2007), pp. 900–909.
[24] H. Kimizuka, H. Kaburaki, and Y. Kogure, *Mechanism for negative Poisson ratios over the $\alpha-\beta$ transition of cristobalite, SiO_2: A molecular-dynamics study*, Phys. Rev. Lett. 84 (2000), pp. 5548–5551.
[25] A. Alderson and K.E. Evans, *Molecular origin of auxetic behavior in tetrahedral framework silicates*, Phys. Rev. Lett. 89 (2002), 225503.
[26] J.N. Grima, R. Gatt, A. Alderson, and K.E. Evans, *An alternative explanation for the negative Poisson's ratios in alpha-cristobalite*, Mater. Sci & Eng. A 423 (2006), pp. 219–224.
[27] J.N. Grima, R. Jackson, A. Alderson, and K.E. Evans, *Do zeolites have negative Poisson's ratios?* Adv. Mater. 12 (2000), pp. 1912–1918.
[28] J.N. Grima, V. Zammit, R. Gatt, A. Alderson, and K.E. Evans, *Auxetic behaviour from rotating semi-rigid units*, Phys. Status Solidi B 244 (2007), pp. 866–882.
[29] J.N. Grima, R. Gatt, V. Zammit, J.J. Williams, K.E. Evans, A. Alderson, and R.I. Walton, *Natrolite: a zeolite with negative Poisson's ratios*, J. Appl. Phys. 101 (2007), 086102.
[30] J.J. Williams, C.W. Smith, K.E. Evans, Z.A.D. Lethbridge, and R.I. Walton, *Off-axis elastic properties and the effect of extraframework species on structural flexibility of the NAT-type zeolites: simulations of structure and elastic properties*, Chem. Mater. 19 (2007), pp. 2423–2434.
[31] C. Sanchez-Valle, S.V. Sinogeikin, Z.A.D. Lethbridge, R.I. Walton, C.W. Smith, K.E. Evans, and J.D. Bass, *Brillouin scattering study*

on the single-crystal elastic properties of natrolite and analcime zeolites, J. Appl. Phys. 98 (2005), 053508.
[32] R.H. Baughman and D.S. Galvao, *Crystalline networks with unusual predicted mechanical and thermal-properties*, Nature 365 (1993), pp. 735–737.
[33] C.B. He, P.W. Liu, P.J. McMullan, and A.C. Griffin, *Toward molecular auxetics: main chain liquid crystalline polymers consisting of laterally attached paraquaterphenyls*, Phys. Status Solidi B 242 (2005), pp. 576–584.
[34] C.B. He, P.W. Liu, and A.C. Griffin, *Toward negative Poisson ratio polymers through molecular design*, Macromolecules 31 (1998), pp. 3145–3147.
[35] P. Aldred and S.C. Moratti, *Dynamic simulations of potentially auxetic liquid-crystalline polymers incorporating swiveling mesogens*, Mol. Simul. 31 (2005), pp. 883–887.
[36] K.L. Alderson and K.E. Evans, *Strain-dependent behaviour of microporous polyethylene with a negative Poisson ratio*, J. Mater. Sci. 28 (1993), pp. 4092–4098.
[37] K.E. Evans and B.D. Caddock, *Microporous materials with negative Poisson's ratios. 2. Mechanisms and interpretation*, J. Phys. D: Appl. Phys. 22 (1989), pp. 1883–1887.
[38] R.H. Baughman, J.M. Shacklette, A.A. Zakhidov, and S. Stafstrom, *Negative Poisson's ratios as a common feature of cubic metals*, Nature 392 (1998), pp. 362–365.
[39] A. Alderson and K.E. Evans, *Microstructural modeling of auxetic microporous polymers*, J. Mater. Sci. 30 (1995), pp. 3319–3332.
[40] A. Alderson and K.E. Evans, *Modelling concurrent deformation mechanisms in auxetic microporous polymers*, J. Mater. Sci. 32 (1997), pp. 2797–2809.
[41] G.Y. Wei, *Design of auxetic polymer self-assemblies*, Phys. Status Solidi B 242 (2005), pp. 742–748.
[42] J.N. Grima, A. Alderson, and K.E. Evans, *Auxetic behaviour from rotating rigid units*, Phys. Status Solidi B 242 (2005), pp. 561–575.
[43] K.V. Tretiakov and K. Wojciechowski, *Poisson's ratio of simple planar 'isotropic' solids in two dimensions*, Phys. Status Solidi B 244 (2007), pp. 1038–1046.
[44] R.F. Almgren, *An isotropic three dimensional structure with Poisson's ratio* $= -1$, J. Elasticity 15 (1985), pp. 427–430.
[45] D. Prall and R.S. Lakes, *Properties of a chiral honeycomb with a Poisson's ratio of* -1, Int. J. Mech. Sci. 39 (1997), pp. 305–314.
[46] A. Spadoni, M. Ruzzene, and F. Scarpa, *Global and local linear buckling behavior of a chiral cellular structure*, Phys. Status Solidi B 242 (2005), pp. 695–709.
[47] K.W. Wojciechowski, *Constant thermodynamic tension Monte Carlo studies of elastic properties of a two-dimensional systems of hard cyclic hexamers*, Mol. Phys. 61 (1987), pp. 1247–1258.
[48] K.W. Wojciechowski and A.C. Branka, *Negative Poisson ratio in a two-dimensional 'isotropic' model*, Phys. Rev. A 40 (1989), pp. 7222–7225.
[49] K.W. Wojciechowski, *Non-chiral, molecular model of negative Poisson ratio in two-dimensions*, J. Phys. A. Math. Gen. 36 (2003), pp. 11765–11778.
[50] J.N. Grima and K.E. Evans, *Auxetic behaviour from rotating squares*, J. Mater. Sci. Lett. 19 (2000), pp. 1563–1566.
[51] Y. Ishibashi and M.J. Iwata, *A microscopic model of a negative Poisson's ratio in some crystals*, J. Phys. Soc. Jpn. 69 (2000), pp. 2702–2703.
[52] J.N. Grima, R. Gatt, A. Alderson, and K.E. Evans, *On the potential of connected stars as auxetic system*, Mol. Simul. 31 (2005), pp. 925–936.
[53] L.J. Gibson, M.F. Ashby, G.S. Schajer, and C.I. Robertson, *The mechanics of two-dimensional cellular materials*, Proc. R. Soc. Lon. A 382 (1982), pp. 25–42.
[54] L.J. Gibson and M.F. Ashby, *Cellular Solids: Structure and Properties*, Pergamon, Oxford, 1988.
[55] J.N. Grima and K.E. Evans, *Auxetic behaviour from rotating triangles*, J. Mater. Sci. 41 (2006), pp. 3193–3196.
[56] J.N. Grima, R. Gatt, P.S. Farrugia, A. Alderson, and K.E. Evans, *Auxetic cellular materials and structures*, in *Proceedings of IMECE 2005*, 2005.
[57] H. Sun, S. Mumby, J. Maple, and A. Hagler, *An* ab-initio *cff93 all-atom force-field for polycarbonates*, J. Am. Chem. Soc. 116 (1994), pp. 2978–2987.
[58] P.P. Ewald, *Die Berechnung optischer und elektrostatischer Gitterpotentiale*, Ann. d. Physik 64 (1921), pp. 253–287.
[59] J.F. Nye, *Physical Properties of Crystals*, Clarendon, Oxford, 1957.
[60] A. Hunter, J. Singh, and J. Thornton, *pi–pi-interactions–The geometry and energetics of phenylalanine phenylalanine interactions in proteins*, J. Mol. Biol. 218 (1991), pp. 837–846.
[61] I.G. Masters and K.E. Evans, *Models for the elastic deformation of honeycombs*, Comp. Struct. 35 (1996), pp. 403–432.